A novel intensity-specific screen identifies RpS21 as a modifier of low-intensity MAPK signaling

Running Title: Low level Ras signaling regulation

Jessica K. Sawyer[1*], Zahra Kabiri[1*], Ruth A. Montague[1], Sarah V. Paramore[1], Erez Cohen[2], Hamed Zaribafzadeh[1], Christopher M. Counter[1,3#], and Donald T. Fox[1,2,3#]

1) Department of Pharmacology & Cancer Biology

2) Department of Cell Biology

3) Duke Cancer Institute

Duke University Medical Center

DUMC Box 3813

Durham, NC 27710

* Contributed equally

#e-mail for correspondence:

chris.counter@duke.edu , don.fox@duke.edu

Key Words: *Drosophila*, Ras, codon bias, RpS21

ABSTRACT

Accumulating evidence suggests the evolutionarily conserved Ras/mitogen activated protein kinase (MAPK) signaling pathway directs distinct biological consequences that depend on distinct intensity states. Given this intensity-dependence, we hypothesized that different levels of Ras/MAPK signaling may be subjected to regulation by different sets of proteins. To identify such 'differential' signaling modifiers, we turned to the *Drosophila* eye as a model. First, we created flies whereby mutant active Ras^{V12} expressed in the eyes was enriched with either rare or commonly occurring codons. We show that this codon manipulation can generate either low or high levels of Ras protein and MAPK signaling, and correspondingly a mild or severe rough-eye phenotype. Using this novel platform to control Ras/MAPK signaling, we performed a whole-genome haploinsufficiency deficiency screen, which yielded 15 deficiencies that modify the rough-eye phenotype in either high or low MAPK signaling states, but not both. We then mapped the underlying gene from one deficiency to the gene *RpS21*. Disrupting *RpS21* expression increases MAPK signaling and enhances the rough-eye phenotype specifically when Ras^{V12} is encoded by rare codons (low signaling), and RpS21 negatively regulates Ras protein and MAPK signaling in several contexts. We also provide evidence that the MAPK pathway promotes expression of RpS21, providing potential negative feedback. Taken together, these data reveal intensity-specific regulation of Ras/MAPK signaling, with the first candidate of this class being RpS21.

INTRODUCTION

The Ras/mitogen activated protein kinase (MAPK) pathway is evolutionarily conserved throughout eukaryotes, serving to transfer external cues to the nucleus to promote a host of cellular responses such as tissue growth and fate determination. Canonical MAPK signaling initiates with the activation of a Receptor Tyrosine Kinase (RTK) by its cognate factor. In turn, this activates the Ras GTPase, by converting it from an inactive GDP-bound to an active GTP-bound conformation. Ras-GTP then activates the MAPK pathway, comprised of Raf kinases, which are activated by Ras and phosphorylate/active Mek kinases, which do the same to Erk kinases. Activation of this cascade then initiates further downstream signaling, often through activation of downstream transcription factors[1]. Dysregulation of the Ras/MAPK pathway is well established to derail a host of biological phenotypes[2]. In humans, weak mutations activating components of this signaling cascade give rise to developmental diseases termed RASopathies[3] while stronger mutations in Ras, Raf, and Mek are well established to cause cancer[4]. Understanding how the Ras/MAPK pathway is regulated thus has important implications not only across evolution, but also with regards to human health.

Recent evidence suggests that the signaling intensity of the Ras/MAPK pathway has biologically important implications. Specifically, expressing the same activating mutant of Mek in either *Drosophila melanogaster* (fruit fly) or *Danio rerio* (zebrafish) was recently shown to either activate or repress Erk phosphorylation depending on the cell type and gene expression environment. These results suggest that special/temporal modifiers of specific Ras/MAPK signaling intensities may drive distinct cellular phenotypes[5]. To gain insight into how this pathway can be employed to induce different cellular responses, we sought to identify factors that modify specific levels of Ras/MAPK signaling in the genetically malleable model organism *Drosophila*. Expression of a mutant active (G12V) *Ras85D* transgene (termed Ras^{V12} here for convenience) in the developing *Drosophila* eye has been successfully employed to screen for modifiers of the

Ras/MAPK pathway[6,7]. Specifically, driving expression of *Ras^{V12}* in the developing eye with an eye-specific promoter such as *sevenless* (*sev*) dysregulates the proper differentiation of the R7 photoreceptor cell, leading to an easily scored 'rough-eye' phenotype. Several screens have identified a host of modifiers of this phenotype, which in turn have identified components as well as regulators of this highly conserved signaling pathway[6–8]. As such, a *Ras^{V12}* modifier approach provides an easily accessible system to screen for intensity-specific or 'differential' Ras/MAPK modifiers.

Critical to screening for such differential modifiers of the Ras/MAPK pathway is a platform to tightly control Ras^{V12} signaling. Here, we introduce an entirely new screening approach to identify intensity-specific *Drosophila* Ras/MAPK modifiers. This approach involves exquisite control of the amount of Ras^{V12} protein produced by changing *Ras* codon usage. Rare codons are well associated with poor translation[9]. We have previously found that changing rare codons in the mammalian Ras isoform *KRAS* to their common counterparts led to elevated translation, protein, signaling, and transformation[10]. We thus posited that expressing the identical Ras^{V12} protein with different codon usage under the identical control of a *sevenless* promoter (using the Gal4/UAS system) introduced into the identical location in the genome would change only one feature- the amount of Ras^{V12} protein produced. Such a system could then be potentially exploited to screen for differential modifiers affecting only one level of Ras^{V12} signaling (high or low intensity). Unlike in *Drosophila* in which there is a single *Ras* gene[11] (flybase: *Ras85D)*, there are three RAS genes in humans, *KRAS*, *NRAS*, and *HRAS*. *KRAS* has the most rare codons, is translated the poorest, yet is mutated the most often in human cancers. This is followed by *NRAS*, whereas *HRAS* is biased towards common codons, is robustly translated but rarely found mutated[10,12]. As the *Drosophila Ras* gene is encoded with mostly common codons, and is more similar to *HRAS*, utilizing a *Ras^{V12}* transgene with a rare codon bias has the added benefit of more closely modeling the most commonly mutated RAS isoform in cancer.

Here, we describe the generation and characterization of transgenic flies and cell lines whereby the degree of Ras^{V12} protein produced, the resultant signaling, and resulting rough-eye phenotype is dictated by the codon usage engineered into the *Ras^{V12}* transgene. We then report the use of flies expressing these transgenes to screen a whole genome deficiency (termed *Df* for convenience) kit for differential modifiers of only low or only high *Ras^{V12}* signaling. Of the 15 *Dfs* identified, we successfully mapped the differential modification of *Df(2L)BSC692*, an enhancer of the rough-eye phenotype of only low Ras^{V12} signaling, to the ribosomal protein S21 gene (*RpS21*). We show that RpS21 negatively regulates Ras protein levels in several contexts, the effect of which is manifested at low levels of signaling. Further, MAPK signaling can also positively regulate RpS21 protein levels, suggesting that RpS21 is part of a negative feedback regulatory loop to tightly control low levels of MAPK signaling. Thus, employing this novel screening platform, we unearthed a novel class of modifiers - those specific to either high or low Ras/MAPK signaling, with the first example being RpS21.

RESULTS

Exploiting codon usage to control the level of MAPK signaling

To screen for signal intensity-specific modifiers of the Ras/MAPK pathway, termed 'differential' modifiers for convenience, we required a platform to tightly control the level of MAPK signaling. We began with the *Drosophila* small GTPase Ras85D, termed Ras here for convenience, as V12 activating mutations in this protein are well established to dominantly activate the MAPK pathway[13,14]. Expressing Ras^{V12} transgenes in the developing eye of *Drosophila* leads to cell fate transformations where cone cells adopt R7 photoreceptor fate, resulting in a "rough-eye" appearance[6,13], an easily scored phenotype that has been extensively capitalized upon to screen for modifiers of the MAPK pathway[6,7,15–17]. To control the level of Ras^{V12} expression, we opted for the novel approach of simply changing the codon usage of the transgene. In more detail, rare codons are known to impede translation, including in *Drosophila*. By choosing rare codons for a given amino acid, it is possible to create an mRNA that is poorly translated without altering the amino acid sequence of the encoded protein. This has the distinct advantage that the control of protein expression is embedded in the DNA and requires no additional factors.

To assess the effect of changing codon usage of constitutively-active Ras^{V12} on the rough-eye phenotype, we used established data on *Drosophila* codon usage (*see* Methods) and created four distinct versions of Ras transgenes: *1*) we altered none of the codons ($Ras^{V12}Native$), *2*) we made all codons the most common ($Ras^{V12}Common$), *3*) we made all codons the most rare ($Ras^{V12}Rare$), and *4*) we created a control wild-type version lacking the V12 mutation and also lacking codon alteration ($Ras^{WT}Native$). To monitor expression, all four transgenes were epitope-tagged at the N-terminus with a 3XFLAG-tag sequence and expressed under the control of a UAS promoter (**Fig1a**, *see* Methods). We note that $Ras^{V12}Native$ has primarily common codons and a

similar Codon Adaptive Index (CAI[18]) to *Ras^{V12}Common*[11], while the CAI for *Ras^{V12}Rare* is much lower (**Figs 1b** and **S1a**). To control for position effects, all transgenes were integrated at the same site in the genome (see Methods).

We first assayed the phenotypic strength of each *Ras* transgene *in vivo* by driving their expression in the developing fly eye using *sevenless (sev)-Gal4*. As expected, expression of *Ras^{WT}* in this manner did not result in a rough-eye phenotype (**Fig1c**). However, when we expressed the constitutive-active versions of *Ras,* we found a range of rough-eye phenotypes **(Fig1c)**. We binned these phenotypes into one of three classes: severe, moderate, or mild. Each class was assigned an increasing numeric score (**Fig1c,** Methods). We then calculated an average severity score for each oncogenic *Ras* transgene. *Ras^{V12}Native* and *Ras^{V12}Common* animals exhibit a similar phenotypic score, reflecting their similar CAI. Further, this phenotypic score was, on average, approximately 2-fold more severe than that of *Ras^{V12}Rare* (**Fig1d**). To determine whether protein levels track with the difference in rough-eye phenotype, we isolated heads from flies encoding the three active *Ras* transgenes in triplicate and immunoblotted with an anti-FLAG antibody. Ras^{V12} levels are similar between *Ras^{V12}Native* and *Ras^{V12}Common* flies, and both are expressed ~2-fold higher than Ras^{V12}*Rare* (**Fig1e** and **S1b**). Given that *Ras^{V12}Native* and *Ras^{V12}Common* produce similar levels of protein and have the same rough-eye phenotype, we opted to control *Ras^{V12}* expression using the *Ras^{V12}Common* and *Ras^{V12}Rare* transgenes.

We next confirmed that *Ras^{V12}Common* and *Ras^{V12}Rare* rough-eye phenotypes were both in the range that can be modified. To this end, we tested known haplo-insufficient modifiers of the Ras/MAPK pathway. Indeed, heterozygous loss-of-function mutations in two known *Ras* suppressors, ***k**inase **s**uppressor of **r**as,* or *ksr*[17], and ***b**eta subunit of type I **g**eranyl***g**eranyl t**r**ansferase*, or *betaggt-I*[7], suppress the rough-eye phenotype for both *Ras^{V12}Common* and *Ras^{V12}Rare* (**Figs 1f** and **S1c**). Conversely, heterozygous loss of the known *Ras* enhancer ***a**nterior **op**en*, or *aop*[19], enhances both the *Ras^{V12}Common* and *Ras^{V12}Rare* rough-eye

phenotypes (**Figs 1f** and **S1c**). These results establish that, as for previously identified *Ras* genetic interactions, the codon-altered Ras^{V12} transgenes are subject to phenotypic modification, including by dose-sensitive haplo-insufficient mutations. To test whether the differential expression of Ras^{V12}*Rare* versus Ras^{V12}*Common* transgenes are capable of altering downstream MAPK signaling, we evaluated the level of activated MAPK signaling in fly heads by measuring the level of phosphorylated Mek (p-Mek, flybase: *Dsor*) and Erk (p-Erk, flybase: *rolled*) compared to the total level of these proteins by immunoblot analysis. Compared to Ras^{V12}*Rare* animals, Ras^{V12}*Common* animals exhibit elevated levels of p-Erk (and to a lesser extent p-MEK) in Ras^{V12}*Common* compared to Ras^{V12}*Rare* fly heads (**Fig1g** and **S1d**). We independently verified this difference in cultured S2 and KC insect cells (*see* Methods), again finding that Ras^{V12}*Common* is expressed higher and more robustly activates the MAPK pathway compared to Ras^{V12}*Rare* (**Figs 1h** and **S1e**). In sum, we find that manipulating codon usage can control the level of Ras^{V12} expression, and in turn, the intensity of MAPK signaling and the corresponding rough-eye phenotype.

A genome-wide screen uncovers differential regulation between high and low Ras/MAPK signaling states

Several haplo-insufficiency modifier screens, including in the eye, have identified new Ras/MAPK signaling regulators[6,14,16,20]. These screens employed the native *Ras* cDNA, which has a strong common-codon bias (**Fig1b**), and as we demonstrate, is similar to Ras^{V12}*Common,* both in terms of high MAPK activation and a severe rough-eye phenotype **(Fig1).** As such, there may be unidentified modifiers of lower intensity MAPK signaling that could be unmasked by driving the rough-eye phenotype with Ras^{V12}*Rare*. To find new Ras/MAPK modifiers, we conducted a genome-wide unbiased haplo-insufficiency screen to specifically identify differential modifiers that either enhance or suppress the rough-eye phenotype driven by only Ras^{V12}*Common* or only Ras^{V12}*Rare* (**Fig 2a**). We used the Bloomington Deficiency (*Df*) Kit, which covers 98.3% of the

euchromatic genome[21]. In a primary screen (**Fig 2b**), we crossed 470 *Dfs* representing 99.1% of the *Df* collection to animals with *Ras^{V12}Rare* or *Ras^{V12}Common* expressed in the eye by a *sev* promoter, and scored the resulting eye severity in an average of 30 (*Ras^{V12}Common*) or 60 (*Ras^{V12}Rare*) progeny animals per cross as in **Fig 1d**.

As expected, we found general *Ras* modifiers that either enhance or suppress both *Ras^{V12}* transgenes (**Fig 2c**) throughout the three autosomes and the X chromosome (**Fig 2d**), although interestingly, we identified more enhancers than suppressors (16% versus 7%, **Fig 2c**). The reason for this remains to be determined, but we note that our calculation of phenotypic modification (see Methods) included scoring animal lethality, which may identify strong enhancers of *Ras^{V12}Common* not identified in previous screens based solely on a rough-eye phenotype. Of great interest, we also identified *Dfs* whereby *Ras^{V12}Common* and *Ras^{V12}Rare* are differentially modified (**Fig 2a**). Using a low-stringency cutoff score (see Methods), we identified 178 putative differential modifier *Dfs* (**Fig 2b**). These *Dfs* were then re-tested by crossing them a second time to *sev-Ras^{V12}Common* and *sev-Ras^{V12}Rare.* We then re-scored the eyes of resulting animals using a more stringent cutoff score (see Methods). This secondary screen (**Fig 2b**) reduced the number of candidates to 15 *Dfs*, or 3% of the tested *Dfs* (**Fig 2c**), that reproducibly differentially modify either only *Ras^{V12}Common* or only *Ras^{V12}Rare* (**Figs 3a**). Among these differential modifiers, we again recovered more enhancers than suppressors, although importantly we recovered both enhancers of *Ras^{V12}Common* and suppressors *Ras^{V12}Rare*, arguing that the screen had the dynamic range to modify both high (*Ras^{V12}Common*) and low (*Ras^{V12}Rare*) intensity Ras/MAPK signaling (**Fig 3b**).

We next queried both the general (intensity-independent) and differential (intensity-dependent) modifiers against a database of known *Ras* genetic interactors (see Methods). 56% of our general modifier *Dfs* covered regions of the genome containing reported *Ras* enhancers or suppressors, validating our approach. Additionally, we note that our screen also identified

potentially new general *Ras* modifiers. Among the differential modifier *Dfs*, most (73%) do not encompass known *Ras* modifiers, supporting the idea that our approach to identify intensity-specific modifier genes also was enriched in novel *Ras* modifiers (**Fig 3c**). To explore possible relationships amongst these 15 differential modifier *Dfs*, we queried the genes within differential versus enhancer and suppressor *Dfs* against the flybase Gene Groups (FBGG). Interestingly, the gene groups enriched in the differential *Dfs* did not overlap with those in the enhancer/suppressor *Dfs* (**Fig 3d**), suggesting that the differential modifiers may form new classes of Ras modifiers. In summary, using the new approach of controlling protein expression of *Drosophila* Ras^{V12} by manipulating codon usage, we successfully identified *Dfs* that alter the rough-eye phenotype in an signaling intensity-specific fashion.

RpS21 negatively regulates Ras/MAPK signaling in an intensity-specific manner

To identify a differential modifier at the gene level, we focused on *Df(2L)*BSC692 as it was one of the smallest deficiencies, encompassing only 12 genes, that specifically enhanced Ras^{V12}*Rare* (**Figs 3a, 4a**). Of these 12 genes, ***R****ibosomal* ***p****rotein* **S21**, or RpS21, stood out as a plausible candidate modifier, as modulating protein levels through canonical or non-canonical ribosome subunit function could be one potential mechanism to reduce MAPK signaling[22]. To determine if *RpS21* was the responsible gene in *Df(2L)BSC692* for specifically enhancing Ras^{V12}*Rare*, we assessed the rough-eye phenotype of Ras^{V12}*Common* and Ras^{V12}*Rare* in the background of the mutant $RpS21^{0375}$ gene. Indeed, only the *sev-*Ras^{V12}*Rare* rough-eye phenotype was enhanced in the $RpS21^{0375}$/+ background (**Fig 4b**).

Given the identification of both an *RpS21* mutant allele and a small deficiency encompassing this gene (*Df(2L)BSC692)* as a differential Ras^{V12} modifier, we next turned our attention to the underlying mechanism of this phenotype. To this end, we measured the level of Ras^{V12} and p-Erk

by immunoblot analysis in four completely distinct settings: ectopic signaling in adult fly heads, ectopic signaling in cultured S2 cells, endogenous signaling in cultured serum-stimulated KC cells, and endogenous signaling in adult fly ovaries. Our results overall closely matched our genetic evidence of a negative regulation of Ras levels and MAPK signaling by RpS21. As in the eye, we found this negative regulation in general to be greater for *Ras* encoded by rare codons, but there were also context-dependent differences to this general finding.

In the heads of *Ras^{V12}Common* versus *Ras^{V12}Rare* flies in a wild-type versus *RpS21^{0375}*/+ background, both transgenic Ras protein and MAPK signaling increase in *RpS21*/+ animals. However, unlike our lack of an observable phenotypic enhancement of *Ras^{V12}Common* in the eye, at the protein level we also observe an increase in the level of Ras^{V12}Common and MAPK signaling in the *RpS21^{0375}*/+ background (**Figs 4c** and **S2a**). This result suggests that RpS21 can indeed modify Ras^{V12}Common levels, but that modification of Ras^{V12}Rare is much more sensitive in terms of altering the eye phenotype. Next, we examined S2 cells transduced with an expression vector encoding either *Ras^{V12}Common* versus *Ras^{V12}Rare* and used RNAi to reduce RpS21 levels. Reducing RpS21 elevates both Ras^{V12}Rare levels and MAPK signaling in *Ras^{V12}Rare* cells. As in our fly eye analysis, we did not observe this effect in *Ras^{V12}Common* cells where RpS21 is reduced. Interestingly, we note that relative to *Ras^{V12}Rare* S2 cells, the level of Ras^{V12} protein and MAPK signaling are substantially elevated even in the presence of RpS21 (**Figs 4d** and **S2b**), perhaps suggesting that Ras signaling is above a threshold of modification in this context.

To further explore the possibility that RpS21 regulates Ras/MAPK signaling independently of Ras codon content, but has a greater effect on Ras in a low signal intensity state, we turned to models of endogenous MAPK signaling. In potential support of the idea that a lower level of Ras/MAPK signaling is susceptible to *RpS21* knockdown irrespective of codons, we examined KC cells. In these cells, endogenous p-Erk is readily detected upon addition of serum following a period of serum starvation. In these cells, we find that upon re-addition of serum (*see* Methods),

RpS21 RNAi elevates endogenous p-Erk levels (**Fig S2c**), again consistent with a negative regulation of the pathway by RpS21. To assess whether endogenous MAPK signaling is regulated by RpS21 *in vivo*, we assessed the effect of disrupting one allele of the *RpS21* gene on endogenous MAPK signaling in the ovaries of flies, a tissue where Erk signaling has a well-defined role[23] and where phosphorylated Mek and Erk are readily detected (**Fig 4e**). In this tissue, endogenous p-Mek and p-Erk levels increase in both *Df(2L)*BSC692/+ and $RpS21^{0375}$/+ ovaries relative to control w^{1118} animals (**Fig 4e**). Together, these findings suggest that Rps21 negatively regulates Ras/MAPK signaling in two endogenous contexts.

Our immunoblot analysis validates our genetic screen finding that RpS21 negative regulates MAPK signaling. However, unlike in our screen, we find that this negative regulation extends beyond codon-dependent effects (**Fig4c, e, Fig S2c**), and potentially depends on the level of signaling (**Fig 4d vs. FigS2c)**. One interpretation of these data is that there is a threshold of MAPK signaling whereby further increases have no effect. Such a model would predict that experimentally reducing the amount of $Ras^{V12}Common$ expression should render fly eye development sensitive to the $RpS21^{0375}$/+ mutant background. To test this threshold model, we took advantage of the fact that expression of transgenes using the Gal4-UAS system is responsive to temperature, with higher temperature resulting in higher expression over the physiological range of 18°C-29°C. In agreement, increasing temperature from 18°C to 29°C causes an observable and significant increase in the phenotypic severity of $Ras^{V12}Common$ (and $Ras^{V12}Native$), but has little effect on $Ras^{V12}Rare$ (**Fig S2d**). These results showed that we could potentially use temperature to test a signaling threshold model. We thus evaluated the rough-eye phenotype of *sev-*$Ras^{V12}Common$ versus *sev-*$Ras^{V12}Rare$ flies in a wild-type versus $RpS21^{0375}$/+ mutant background, only this time at 18°C. At this lower temperature, *RpS21/+* now acts as an enhancer of $Ras^{V12}Common$ (**Fig 4f**). Interestingly, *RpS21/+* no longer enhances $Ras^{V12}Rare$, underscoring the sensitivity of *RpS21/+* to Ras/MAPK signaling output. Collectively, these results

demonstrate that while RpS21 negatively regulates Ras-MAPK signaling in diverse contexts, at the phenotypic level this regulation preferentially impacts low level Ras/MAPK signaling.

A potential negative feed-back loop involving RpS21

There is a precedent for the MAPK pathway controlling expression of its negative regulators, or feedback control[24,25]. To investigate whether RpS21 was similarly regulated by the MAPK pathway, we compared the level of RpS21 protein when this pathway was activated in S2 cells by expression of activated Mek^{EE}, Ras^{V12}, or Raf^{ED}. All three forms of activating the MAPK pathway elevate levels of RpS21 (**Figs 5a,b** and **S3a,b**). We validated these results in the opposite direction, namely demonstrating that the high levels of RpS21 induced by *Ras^{V12}Common* or *Ras^{V12}Rare* in KC cells is reduced by treatment with the Mek inhibitor Trametinib (**Figs 5c** and **S3c**). *In vivo*, RpS21 levels are higher in heads of *sev-Ras^{V12}Common* compared to *sev-Ras^{V12}Rare* flies (**Figs 5d** and **S3d**), again consistent with a positive relationship between MAPK activation and RpS21 levels.

The above results suggest that, as Ras/MAPK activation rises, so will RpS21 levels, which will then feedback to inhibit Ras/MAPK activation. To test this idea, we took advantage of our serum re-addition model in KC cells to explore the relationship of endogenous MAPK signaling and RpS21 levels in a temporal manner. We thus examined the amount of RpS21 expressed by immunoblot analysis when the MAPK pathway was stimulated in serum-starved KC cells by the addition of serum, as above. As expected, addition of serum causes a rapid increase in p-Mek followed by p-Erk levels, which was mirrored by an increase in RpS21 levels (**Figs 5e** and **S3e**). These results are consistent with our findings that the MAPK pathway stimulates the RpS21 expression. Interestingly, after RpS21 levels reach their peak, there is a reduction in p-Mek and p-Erk, again consistent with RpS21 suppressing MAPK signaling, which is coincident with a

reduction in RpS21 levels (**Figs 5e and S3e**). We note here that the timing of when RpS21 reached peak expression after serum stimulation varied from experiment to experiment and was influenced by cell type, but typically tracked with p-Mek and p-Erk levels (not shown). At later time points, both RpS21 and MAPK activity levels again rise (**Figs 5e and S3e**), which may reflect the known oscillatory nature of MAPK signaling[26]. Collectively, these data support a model whereby RpS21 acts as both a negative regulator and effector of the MAPK pathway in a signal intensity-dependent fashion (**Fig 5f**).

DISCUSSION

Here, we demonstrate that by manipulating codon usage it is possible to control the expression, signaling, and a biological phenotype of driven by active Ras/MAPK. We exploited this approach to screen for modifiers of high versus low MAPK signaling intensity, and report the identification of 15 *Df* from a whole-genome screen that either enhanced or suppressed the rough-eye phenotype driven by either a common or rare codon-enriched Ras^{V12} transgene, but not both. Further, we report that in one such *Df*, *Df(2L)BSC692*, the underlying gene mapped to the *RpS21* gene. Disrupting *RpS21* expression increases MAPK signaling in several contexts and enhances the rough-eye phenotype specifically of *sev-*Ras^{V12}*Rare* flies. We also provide evidence that the MAPK pathway increases the expression of RpS21, suggesting a potential negative feedback loop relationship between Ras/MAPK signaling and RpS21.

Our results show that the ability to control protein expression by altering codon usage is a valuable platform to stably alter protein production to undertake signal intensity-specific screens. Such an approach may find use in interrogating other pathways in a similar manner. As mentioned, the described screen yielded 15 differential modifiers, which largely contain genes not previously linked to Ras signaling, which speaks to the novel utility of this approach to identify new modifiers. While the identity of the genes responsible for the differential phenotype in each *Df*, with the exception of *DF(2L)BSC692*, remain to be mapped, these *Dfs* nevertheless represent a rich source of potentially new genes modulating Ras/MAPK signaling. Given the importance of this pathway in many settings across evolution, such modifiers may shed important insight into how this pathway is controlled at different levels of signaling intensities. It is worth noting that: 1) weak activating mutations in the MAPK pathway of humans underlie a class of human diseases termed RASopathies[3], and 2) the weakest expressed mammalian RAS isoform, *KRAS*[10] is the most commonly mutated RAS isoform in human cancers[12]. As such, modifiers of low-intensity Ras signaling may provide a new class of proteins to explore in these diseases.

As mentioned, RpS21 functions as a negative regulator of low Ras/MAPK signaling, potentially by suppressing the level of Ras protein. Interestingly, downregulation of RpS21 was previously shown to cause excessive hyperplasia in hematopoietic organs and imaginal disc overgrowth during larval development, suggesting RpS21 acts as tumor suppressor in *Drosophila*[22]. Haploinsufficiency of many ribosomal proteins has also been reported to be tumorigenic in zebrafish[27], and heterozygous inactivating mutations of ribosomal proteins have been described in human cancers[28,29]. Several mechanisms have been proposed to account for this apparent tumor suppressor activity including activation of p53[30–32], inhibition of NF-κB[33], E2F[34], MYC[35], and CDK8[36]. Thus, RpS21 joins the ranks of the emerging appreciation for a role of ribosomal proteins in tumorigenesis, although whether RpS21 acts as a tumor suppressor in mammals awaits investigation.

RpS21 heterozygous inactivation was associated with elevated Ras^{V12} protein, but admittedly how this is achieved remains to be elucidated. The effect of RpS21 on Ras^{V12} protein level could potentially be through RpS21 ribosomal or extra ribosomal function. A defect in RpS21 ribosomal function may trigger ribosomal biogenesis defects that alter translational fidelity or promote generation of oncoribosomes to preferentially express subset of mRNA pools[37,38]. Alternatively, RpS21 might also involve in other cellular processes independent of its canonical ribosomal function, as has been shown for other ribosomal subunits[39,40].

The Ras/MAPK signaling is tightly controlled by positive and negative regulators to maintain certain signaling thresholds or outputs required for different cellular processes[25]. Indeed, many of negative regulators of Ras/MAPK signaling are involved in feedback loops and are conserved in *Drosophila*, *C elegans*, and humans[24,41–44]. In this regard, we present evidence that RpS21 not only suppresses Ras/MAPK signaling, but that Ras/MAPK signaling stimulates RpS21 production. This suggests the intriguing possibility that RpS21 is a negative regulator of the Ras/MAPK pathway as part of a negative feedback loop, although this remains to be thoroughly

investigated. Related to this, another question for future investigation is why the potential negative feedback loop is non-functional at high-intensity levels of Ras/MAPK signaling, like we observed in S2 cells. One possible explanation is that different MAPK signaling states activate a different host of MAPK targets, and this impacts the degree of negative regulation by RpS21. To that end, it will be important to further mine our screen to identify single gene modifiers in the other 14 *Dfs*, which may similarly yield new regulatory insight into the Ras/MAPK pathway.

METHODS

Generation of codon-altered Ras^{V12} genes in Drosophila

Codon-altered exon sequences for *Ras^{V12}Common* and *Ras^{V12}Rare* were created using the Kazusa codon usage database (https://www.kazusa.or.jp/codon/) and subsequently generated by Invitrogen GeneArt Gene Synthesis (ThermoFisher Scientific). A cDNA clone (LD17536, Drosophila Genomics Resource Center) was used as a template to generate the non-altered *Ras85D* sequence. To generate *Ras^{V12}Native*, the QuikChange II Site-Directed Mutagenesis Kit (Agilent) was used to change codon 12 in *Ras85D* from GGA (glycine) to GTA (valine). Subsequently, primers (available upon request) were designed to amplify *Ras* sequences and the Invitrogen Gateway BP Clonase II Enzyme Mix (ThermoFisher Scientific) was used to insert these sequences into the Gateway entry vector pDONOR221 (ThermoFisher Scientific). Subsequently, the Invitrogen LR Clonase Enzyme Mix (ThermoFisher Scientific) was used to insert the Ras85D, Native, Common, and Rare sequences into the Gateway destination vector pBID-UASC-FG (Addgene Plasmid #3520[45]), which has a N-terminal FLAG tag and a PhiC31 site for site-directed genomic insertion. pBID-UASC-FG-*Ras* plasmids were prepared with a ZymoPURE II Plasmid Midiprep Kit (Zymo Research) and sent to Model System Injections (Durham, NC, USA) for injection into *attP40 (2L)* flies. For cell culture, *Ras^{V12}Common* and *Ras^{V12}Rare* transgenes were cloned into pMKInt-Hyg vectors, which were sequenced to confirm the correct sequence.

Codon Usage

To determine the Codon Adaptive Index (CAI), sequences were entered at the CAIcal web-server (http://genomes.urv.es/CAIcal[46].

Fly stocks

All flies were raised at 25°C on standard media unless noted otherwise (Archon Scientific, Durham NC). Flybase (http://flybase.org) describes full genotypes for the following stocks used in this study from the Bloomington Drosophila Stock Center: *ksr*$^{S\text{-}627}$*/TM3,Sb* (#5683), *aop*$^{yan\text{-}XE18}$*/CyO* (#8777), *betaggt-I*$^{S\text{-}2554}$ (#5681), *RpS21*^{03575}*/CyO* (#11339), and the Bloomington Deficiency(Df) kit. The following stocks were generated for this study: *UAS-FLAG-Ras85D*, *UAS-FLAG-Ras*^{V12}*Native*, *UAS-FLAG-Ras*^{V12}*Common*, and *UAS-FLAG-Ras*^{V12}*Rare*.

Fly Genetics and Deficiency Screen

The *Ras* transgenes were combined with a *sev*Gal4 driver and subsequently crossed to *Df*/Balancer flies. After 18-20 days, the rough eye phenotype of the resulting progeny was scored. The scoring system was as follows (category=numerical score, qualitative description): Mild=1, no discoloration or necrotic tissue; Moderate=3, discoloration and no necrotic tissue; Severe=5, discoloration and necrotic tissue (see **Fig1c,d**). Severity scores for each genotype was calculated as follows: (#Mildx1+#Moderatex3+#Severex5)/Total # of flies. To determine if haploinsufficiency for a subset of genes altered the rough eye phenotype the following two genotypes for each deficiency (*Df*) were compared: *Ras* transgene only and *Ras* transgene + *Df* (used as an internal comparison to control for background effects). Then, we calculated a fold change score for both *Ras*^{V12}*Common* and *Ras*^{V12}*Rare* for each deficiency: *Ras* transgene + deficiency/*Ras* transgene. For the primary screen, the fold change score was defined as follows: enhancer (fold change ≥1.35 or 5X more flies eclosed); suppressor (fold change ≤0.65 or 5X less flies eclosed). For the secondary screen, the fold change score was defined as follows: enhancer (fold change ≥1.95 or 5X more flies eclosed); suppressor (fold change ≤0.50 or 5X less flies eclosed). The final phenotype for a deficiency was defined as follows: not a modifier (neither *Ras*^{V12}*Common* or *Ras*^{V12}*Rare* + *Df* were modified); enhancer (both *Ras*^{V12}*Common* and *Ras*^{V12}*Rare* + *Df* were

enhanced); suppressor (both *Ras^{V12}Common* and *Ras^{V12}Rare + Df* were enhanced); differential (only *Ras^{V12}Common* or *Ras^{V12}Rare + Df* were modified).

Imaging

Images of fly eyes were obtained using a Leica MZ10F microscope with a PlanApo 1.6X objective, Pixel Shift Camera DMC6200, and LASX software.

Protein Preparation and Analysis

Drosophila protein samples were prepared by homogenizing tissue on ice.

For Fig1e, samples were processed in Laemmli buffer and then boiled for 5min. Samples were separated by 12% SDS-PAGE and transferred to an Odyssey nitrocellulose membrane (LI-COR Biosciences) for immunoblotting. The following antibodies were used: FLAG M2 (1:500, Sigma, anti-mouse), α-tubulin (1:20,000, Sigma, anti-mouse), IRDye 800CW (1:20,000, LI-COR Biosciences, anti-mouse). Signal was detected using LI-COR Odyssey CLx and analyzed using Image Studio (LI-COR Biosciences).

For all other immunoblots, samples were processed in RIPA buffer containing 1% IGEPAL, 50mM NaCl, 2mM EDTA, 100mM Tris-HCl, pH 8.0, 0.1% Glycerol, 50 mM Naf, 10mM Na3VO4, and protease inhibitors (Roche). *Drosophila* heads and ovaries were collected and transferred to cold lyses to be homogenized with a pellet pestle. Lysates were incubated at 4 °C for 30 min on end-to-end rotator and then centrifuged at 21,000 x g for 10 min. The supernatant was transferred to a new tube to be used for the next step. Total protein was quantified using a BCA kit (Bio-Rad) and either 30 or 50 microgram of protein was used for separation on either 12.5% or 15% gradient sodium dodecyl sulfate-polyacrylamide electrophoresis (SDS-PAGE) gels. Proteins on SDS gels were transferred onto polyvinylidene difluoride membranes. These membranes were probed with anti-Flag (Sigma #F1804 anti-mouse 1:1000) or β-actin (Cell Signaing #4967; 1:1000), p-MEK1/2

(Cell Signaling #9121, 1:500), MEK1/2 (Cell Signaling # 9122, 1;500), p-ERK1/2 (Cell Signaling #9101, 1:1000), ERK1/2 (Cell Signaling # 4695, 1:1000), RPS21 (Abcam #ab90874, 1:2000), Pyo (anti-Glu-Glu) (VWR #10715-199, 1:500) primary antibodies in blocking buffer containing 5% milk followed by the secondary antibodies of goat anti-mouse IgG (H+L) HRP (Life Technologies, #G21040, 1:10000) or goat anti-rabbit IgG (H+L) HRP (Thermo Fisher Scientific, #65-6120, 1:10000) . Immunoblots were visualized using Clarity Max^{TM} ECL Western Blotting Detection Reagent (Bio-Rad #1705062) followed by exposure to digital acquisition using Chemi Doc Imager (Bio-Rad). For all blots, the contrast and/or brightness were altered equally across the entire image and then images were cropped for displaying as figures.

Cell Culture

KC and S2 cell lines were obtained from Bloomington (Indiana University DGRC Bloomington) and as a gift from Dr. MacAlpine respectively. These cells were cultured in Schneider *Drosophila* medium (Invitrogen #21720-024) supplemented with 10% fetal bovine serum (FBS) and 1% penicillin–streptomycin- L Glutamine (Invitrogen #10378-016) at 25°C. FBS was heated for 60 minutes in 58°C and then cool down before added to medium. These cells were confirmed to be free of mycoplasma infection, as measured by the Duke Cell Culture Facility using MycoAlert PLUS test (Lonza). S2 and KC cell lines were stably transduced with the pMKInt-Hyg vector encoding *Ras^{V12}Common* and *Ras^{V12}Rare* cDNAs using 1000 ng of DNA in 6 well plates as instructed by Effectene transfection reagent (Qiagen, #301425). The following day, Schneider media was changed, and cells were seeded in a coated culture dish (100x20 mm). Four days later, cells were passaged with fresh Schneider medium and 200 µg/ ml hygromycin (Invitrogen #10687-010) was added. The stably transfected cells were selected within a month growing in media containing hygromycin. Three days prior to any experiment, these cells were grown in media without hygromycin.

S2 cells were transiently transfected with either pMet-HA-Ras^{V12}, pMet-pyo-Raf^{ED}, and pMet-myc-Mek^{EE} vectors (kindly provided by Dr. Marc Therrien[47]) using the Effectene transfection reagent as described above. Two days later, these cells were treated with 500 µM CuSO4 for 16 hours to include expression of transgene. Four million S2 cells that are stably transduced with *Ras^{V12}Common* and *Ras^{V12}Rare* plasmids were seated into coated tissue culture dishes (60x15mm, VWR #25382-188) with 2 ml of Schneider media (without FBS). Sixty micrograms of RpS21 dsRNA were added on top of these cells. One hour later, two ml Schneider media containing 20% FBS were added on top of 2 ml Schneider media without FBS resulting in medium with 10% FBS concentration in total media of this culture. Within 16-24 hours after RNAi treatment, expression of *Ras^{V12}Common* and *Ras^{V12}Rare* transgenes were induced by CuSO4 for another 12 hours. Finally, these cells were collected 30-36 hours after dsRNA treatment. KC cells *Ras^{V12}Common* and *Ras^{V12}Rare* were treated with 10 nM trametinib for 12- 16 hours prior collecting for immunoblot assay.

dsRNA synthesis

S2 cell DNA was used to produce a PCR template for RpS21 dsRNA production using the forward primer "TAATACGACTCACTATAGGGTTACTGACCAGCCGATACCC" and reverse primer "TAATACGACTCACTATAGGGCCACGCTTAGAAGTTCCTGC". Next, 500 ng RpS21 PCR template was used for an *in vitro* production of dsRNA as instructed in the MEGAscrip T7 transcription kit (ThermoFisher #AM1334). The dsRNA solution was cleared using MegaClear^{TM} kit (ThermoFisher #AM1908). Finally, the concentration of RpS21 dsRNA was measured and stored in -80°C for future use.

Gene enrichment analysis

Deficiency sequence boundaries were defined using coordinates available through flybase[48] and Bloomington *Drosophila* Stock Center. Deficiencies were then uploaded as a custom BED track to UCSC Genome Browser (Reference Assembly ID: dm6). Genes overlapping the

deficiency coordinates were then extracted using BEDtools for additional analysis[49]. A deficiency was determined to contain known RAS modifiers if any of the deficiency covered genes known as *Drosophila* RAS85D genetic interactors (332 interactors, flybase). Enhancers and suppressor deficiencies were analyzed using the same metric against known RAS85D interactors of the same respective modifier type. Statistical analysis (chi-square) was performed using Graphpad Prism v8.1. flybase Gene Group Enrichment analysis was performed by comparing deficiency covered genes with pre-defined flybase Gene Groups. Analysis and statistical tests were performed in R using Gene Overlap package (https://rdrr.io/bioc/GeneOverlap/) and results are reported as adjusted p-values (False Discovery Rate[50]).

Statistical Analysis and Reporting

Graphs and statistical analysis were generated using GraphPad Prism 7. Statistical tests and P-values are detailed in figure legends. For all tests, P-value reporting is as follows: (P>0.05, n.s.); P<0.05,*); (P<0.01,**); (P<0.001,***), (P<0.0001,****).

REFERENCES

1. Patel, A. L. & Shvartsman, S. Y. Outstanding questions in developmental ERK signaling. *Development* (2018). doi:10.1242/dev.143818

2. Goyal, Y., Schüpbach, T. & Shvartsman, S. Y. A quantitative model of developmental RTK signaling. *Developmental Biology* (2018). doi:10.1016/j.ydbio.2018.07.012

3. Rauen, K. A. The RASopathies. *Annu. Rev. Genomics Hum. Genet.* (2013). doi:10.1146/annurev-genom-091212-153523

4. Jindal, G. A. *et al.* In vivo severity ranking of Ras pathway mutations associated with developmental disorders. *Proc. Natl. Acad. Sci.* (2017). doi:10.1073/pnas.1615651114

5. Goyal, Y. *et al.* Divergent effects of intrinsically active MEK variants on developmental Ras signaling. *Nat. Genet.* **49**, 465–469 (2017).

6. Karim, F. D. *et al.* A screen for genes that function downstream of Ras1 during Drosophila eye development. *Genetics* **143**, 315–329 (1996).

7. Maixner, A., Hecker, T. P., Phan, Q. N. & Wassarman, D. A. A screen for mutations that prevent lethality caused by expression of activated sevenless and ras1 in the Drosophila embryo. *Dev. Genet.* **23**, 347–361 (1998).

8. Therrien, M., Morrison, D. K., Wong, A. M. & Rubin, G. M. A genetic screen for modifiers of a kinase suppressor of Ras-dependent rough eye phenotype in Drosophila. *Genetics* **156**, 1231–1242 (2000).

9. Quax, T. E. F., Claassens, N. J., Söll, D. & van der Oost, J. Codon Bias as a Means to Fine-Tune Gene Expression. *Mol. Cell* (2015). doi:10.1016/j.molcel.2015.05.035

10. Lampson, B. L. *et al.* Rare Codons Regulate KRas Oncogenesis. *Curr. Biol.* **23**, 70–75

(2013).

11. Neuman-Silberberg, F. S., Schejter, E., Hoffmann, F. M. & Shilo, B. Z. The Drosophila ras oncogenes: structure and nucleotide sequence. *Cell* **37**, 1027–1033 (1984).

12. Hobbs, G. A., Der, C. J. & Rossman, K. L. RAS isoforms and mutations in cancer at a glance. *J. Cell Sci.* (2016). doi:10.1242/jcs.182873

13. Fortini, M. E., Simon, M. A. & Rubin, G. M. Signalling by the sevenless protein tyrosine kinase is mimicked by Ras1 activation. *Nature* **355**, 559–561 (1992).

14. Gaul, U., Mardon, G. & Rubin, G. M. A putative Ras GTPase activating protein acts as a negative regulator of signaling by the Sevenless receptor tyrosine kinase. *Cell* **68**, 1007–1019 (1992).

15. Dickson, B. J., van der Straten, A., Dom\'\inguez, M. & Hafen, E. Mutations Modulating Raf signaling in Drosophila eye development. *Genetics* **142**, 163–171 (1996).

16. Gaul, U., Chang, H., Choi, T., Karim, F. & Rubin, G. M. Identification of ras targets using a genetic approach. *Ciba Found. Symp.* **176**, 85–92– discussion 92–5 (1993).

17. Therrien, M. *et al.* KSR, a novel protein kinase required for RAS signal transduction. *Cell* **83**, 879–888 (1995).

18. Sharp, P. M. & Li, W. H. The codon adaptation index-a measure of directional synonymous codon usage bias, and its potential applications. *Nucleic Acids Res.* (1987). doi:10.1093/nar/15.3.1281

19. Rebay, I. & Rubin, G. M. Yan functions as a general inhibitor of differentiation and is negatively regulated by activation of the Ras1/MAPK pathway. *Cell* **81**, 857–866 (1995).

20. Rørth, P. A modular misexpression screen in Drosophila detecting tissue-specific

phenotypes. *Proc. Natl. Acad. Sci. U. S. A.* **93**, 12418–22 (1996).

21. Cook, R. K. *et al.* The generation of chromosomal deletions to provide extensive coverage and subdivision of the Drosophila melanogaster genome. *Genome Biol.* **13**, R21 (2012).

22. Török, I. *et al.* Down-regulation of RpS21, a putative translation initiation factor interacting with P40, produces viable minute imagos and larval lethality with overgrown hematopoietic organs and imaginal discs. *Mol. Cell. Biol.* **19**, 2308–2321 (1999).

23. Cheung, L. S., Schüpbach, T. & Shvartsman, S. Y. Pattern formation by receptor tyrosine kinases: Analysis of the Gurken gradient in Drosophila oogenesis. *Current Opinion in Genetics and Development* (2011). doi:10.1016/j.gde.2011.07.009

24. Dougherty, M. K. *et al.* Regulation of Raf-1 by direct feedback phosphorylation. *Mol. Cell* (2005). doi:10.1016/j.molcel.2004.11.055

25. Lake, D., Corrêa, S. A. L. & Müller, J. Negative feedback regulation of the ERK1/2 MAPK pathway. *Cellular and Molecular Life Sciences* (2016). doi:10.1007/s00018-016-2297-8

26. Shankaran, H. *et al.* Rapid and sustained nuclear-cytoplasmic ERK oscillations induced by epidermal growth factor. *Mol. Syst. Biol.* (2009). doi:10.1038/msb.2009.90

27. Amsterdam, A. *et al.* Many ribosomal protein genes are cancer genes in zebrafish. *PLoS Biol.* (2004). doi:10.1371/journal.pbio.0020139

28. Ajore, R. *et al.* Deletion of ribosomal protein genes is a common vulnerability in human cancer, especially in concert with TP53 mutations . *EMBO Mol. Med.* (2017). doi:10.15252/emmm.201606660

29. Russo, A. & Russo, G. Ribosomal proteins control or bypass p53 during nucleolar stress.

International Journal of Molecular Sciences (2017). doi:10.3390/ijms18010140

30. Chen, J., Guo, K. & Kastan, M. B. Interactions of nucleolin and ribosomal protein L26 (RPL26) in translational control of human p53 mRNA. *J. Biol. Chem.* **287**, 16467–16476 (2012).

31. Sloan, K. E., Bohnsack, M. T. & Watkins, N. J. The 5S RNP Couples p53 Homeostasis to Ribosome Biogenesis and Nucleolar Stress. *Cell Rep.* (2013). doi:10.1016/j.celrep.2013.08.049

32. Donati, G., Peddigari, S., Mercer, C. A. & Thomas, G. 5S Ribosomal RNA Is an Essential Component of a Nascent Ribosomal Precursor Complex that Regulates the Hdm2-p53 Checkpoint. *Cell Rep.* (2013). doi:10.1016/j.celrep.2013.05.045

33. Wan, F. *et al.* Ribosomal Protein S3: A KH Domain Subunit in NF-κB Complexes that Mediates Selective Gene Regulation. *Cell* (2007). doi:10.1016/j.cell.2007.10.009

34. Donati, G. *et al.* Selective inhibition of rRNA transcription downregulates E2F-1: a new p53-independent mechanism linking cell growth to cell proliferation. *J. Cell Sci.* (2011). doi:10.1242/jcs.086074

35. Barna, M. *et al.* Suppression of Myc oncogenic activity by ribosomal protein haploinsufficiency. *Nature* **456**, 971–975 (2008).

36. Lessard, F. *et al.* Senescence-associated ribosome biogenesis defects contributes to cell cycle arrest through the Rb pathway. *Nat. Cell Biol.* (2018). doi:10.1038/s41556-018-0127-y

37. Shi, Z. *et al.* Heterogeneous Ribosomes Preferentially Translate Distinct Subpools of mRNAs Genome-wide. *Mol. Cell* (2017). doi:10.1016/j.molcel.2017.05.021

38. Lessard, F., Brakier-Gingras, L. & Ferbeyre, G. Ribosomal Proteins Control Tumor Suppressor Pathways in Response to Nucleolar Stress. *BioEssays* (2019). doi:10.1002/bies.201800183

39. Warner, J. R. & McIntosh, K. B. How Common Are Extraribosomal Functions of Ribosomal Proteins? *Molecular Cell* (2009). doi:10.1016/j.molcel.2009.03.006

40. Dionne, K. L., Bergeron, D., Landry-Voyer, A. M. & Bachand, F. The 40S ribosomal protein uS5 (RPS2) assembles into an extraribosomal complex with human ZNF277 that competes with the PRMT3– uS5 interaction. *J. Biol. Chem.* (2019). doi:10.1074/jbc.RA118.004928

41. Matallanas, D. *et al.* Raf family kinases: Old dogs have learned new tricks. *Genes and Cancer* (2011). doi:10.1177/1947601911407323

42. Douziech, M., Sahmi, M., Laberge, G. & Therrien, M. A KSR/CNK complex mediated by HYP, a novel SAM domain-containing protein, regulates RAS-dependent RAF activation in Drosophila. *Genes Dev.* (2006). doi:10.1101/gad.1390406

43. Therrien, M., Wong, A. M. & Rubin, G. M. CNK, a RAF-binding multidomain protein required for RAS signaling. *Cell* (1998). doi:10.1016/S0092-8674(00)81766-3

44. Kornfeld, K., Hom, D. B. & Horvitz, H. R. The ksr-1 gene encodes a novel protein kinase involved in Ras-mediated signaling in C. elegans. *Cell* (1995). doi:10.1016/0092-8674(95)90206-6

45. Wang, J.-W., Beck, E. S. & McCabe, B. D. A modular toolset for recombination transgenesis and neurogenetic analysis of Drosophila. *PLoS One* **7**, e42102 (2012).

46. Puigbò, P., Bravo, I. G. & Garcia-Vallve, S. CAIcal: A combined set of tools to assess

codon usage adaptation. *Biol. Direct* (2008). doi:10.1186/1745-6150-3-38

47. Ashton-Beaucage, D. *et al.* A Functional Screen Reveals an Extensive Layer of Transcriptional and Splicing Control Underlying RAS/MAPK Signaling in Drosophila. *PLoS Biol.* (2014). doi:10.1371/journal.pbio.1001809

48. Thurmond, J. *et al.* FlyBase 2.0: the next generation. *Nucleic Acids Res.* (2018). doi:10.1093/nar/gky1003

49. Quinlan, A. R. & Hall, I. M. BEDTools: A flexible suite of utilities for comparing genomic features. *Bioinformatics* (2010). doi:10.1093/bioinformatics/btq033

50. Benjamini, Y. & Hochberg, Y. Controlling the False Discovery Rate: A Practical and Powerful Approach to Multiple Testing. *J. R. Stat. Soc. Ser. B* (1995). doi:10.1111/j.2517-6161.1995.tb02031.x

FIGURE LEGENDS

Figure 1. Exploiting codon usage to control the level of MAPK signaling. (a) Schematic representation of the FLAG epitope-tagged *Ras*^{V12} transgenes encoded by rare, common, or native codons. A WT (non-V12 version with native codons) was also generated, but is not shown here. **(b)** Codon Adaptive Index (CAI) plot. Transparent circles, squares, and triangles are individual CAIs per codon. Solid lines represent a best-fit line of individual points for each transgene. **(c)** Images representing the phenotypes assessed and the scoring system. Scale bars = 0.5mm. **(d)** The mean ± SEM severity score of the indicated *Ras*^{V12} transgenes from three replicate experiments at 25°C. **(e)** Immunoblot detection transgenic Ras^{V12} protein (with an anti-FLAG antibody) and αTubulin as a loading control from lysates derived from the head of flies with the indicated versions of transgenic *Ras*^{V12}. **(f)** Quantification of severity scores for *Ras* transgenes that are also haploinsufficient for known *Ras* modifiers. Data represent mean ± SEM, multiple replicates. **(g,h)** Immunoblot detection of transgenic Ras^{V12} (with an anti-FLAG antibody), phosphorylated (p-) and total Mek and Erk, and actin as a loading control from lysates derived from **(g)** the head of flies with the indicated versions of transgenic *Ras*^{V12} or **(h)** S2 cells stably transduced with expression vectors expressing the indicated *Ras*^{V12} transgenes. Tukey's multiple comparisons test was used for statistical comparisons. ****p<0.0001. ***p<0.001. **p<0.01. n.s., not significant.

Figure 2. A genome-wide screen uncovers differential regulation between high and low Ras/MAPK signaling states.

(a) Schematic of the *Ras* modifiers types scored in the *Df* screen. **(b)** Schematic of screening approach. **(c)** Pie chart showing the number of *Df* with the indicated types of *Ras* modifiers. **(d)** **(e)** Genome map of deficiencies color coded as in c for the class of *Ras* modifier.

Figure 3. Characterization of differential modifiers. (a) Characterization of the differential *Ras* modifiers identified. Asterisks= those *Df*s for which no known *Ras* modifier has been reported (see Methods). **(b)** Pie chart showing the number of differential modifiers with the indicated phenotypes. **(c)** Graph of the percent (and number) of *Dfs* that do or do not contain known Ras interacting genes. **(d)** Enriched flybase gene groups contained in differential versus enhancer and suppressor deficiencies.

Figure 4. RpS21 negatively regulates Ras/MAPK signaling in an intensity-specific manner. (a) Genome map of *Df(2L)BSC692*. *RpS21* is highlighted in green. **(b,f)** The mean ± SEM severity score of the genotypes from three replicate experiments at **(b)** 25°C or **(f)** 18°C. **(c,d,e)** Immunoblot detection of transgenic Ras^{V12} (with an anti-FLAG antibody), phosphorylated (p-) and total Mek and/or Erk, RpS21, and actin as a loading control from lysates derived from **(c)** the head of flies with the indicated versions of transgenic Ras^{V12} in either the wild-type (+/+) or mutant ($RpS21^{0375}$/+) RpS21 backgrounds, **(d)** S2 cells stably transduced with expression vectors expressing the indicated Ras^{V12} transgenes in the absence (-) and presence (+) of *RpS21* RNAi, or **(e)** the ovaries of either wild-type (+/+) or mutant ($RpS21^{0375}$/+) RpS21 flies. Tukey's multiple comparisons test was used for statistical comparisons. ****p<0.0001. **p<0.01. n.s., not significant.

Figure 5. A potential negative feed-back loop involving RpS21. (a,b) Immunoblot detection of Ras, Mek, RpS21, Raf, or actin as a loading control in S2 cells stably transduced with expression vectors expressing **(a)** no transgene (-), activated Mek^{EE}, or activated Ras^{V12} or **(b)** no transgene (-) or activated Raf^{DD} (anti-pyo antibody to detect tagged pyo-Raf^{ED}). **(c)** Immunoblot detection of transgenic Ras^{V12} (with an anti-FLAG antibody), phosphorylated (p-) and total Erk, RpS21, and actin as a loading control from lysates derived from KC cells stably transduced with

expression vectors expressing the indicated *Ras*^{V12} transgenes in the absence (-) and presence of the Mek inhibitor trametinib (Tram). **(d**) Immunoblot detection of transgenic Ras^{V12} (with an anti-FLAG antibody), RpS21, and actin as a loading control from lysates derived from the head of flies with the indicated versions of transgenic *Ras*^{V12}. **(e)** Immunoblot detection of phosphorylated (p-) and total Mek and Erk, RpS21, and actin as a loading control from lysates derived from serum-starved KC cells at the indicated times after stimulation with fetal bovine serum (FBS). **(f)** Proposed model of the effect of RpS21 on different levels of MAPK signaling.

Supplementary Figures

Figure S1. **Codon manipulation of *Ras*^{V12} promotes differential MAPK signaling intensity in *Drosophila*. (a)** Alignments of *Ras* transgenes. Nucleotide changes highlighted for *Ras*^{V12}*Common* (red) and *Ras*^{V12}*Rare* (blue). Table with overall CAI score and GC content for *Ras* transgenes. (**b)** Quantification of protein levels at 25°C for blot in **Fig 1e**. Data represent mean ± SEM, 3 replicates, Tukey's multiple comparisons test. **(c)** Table showing the average number of flies eclosed per experiment in **Fig 1f** for Rare and Common transgenes in a known *Ras* modifier background. **(d)** Immunoblot detection of transgenic Ras^{V12} (with an anti-FLAG antibody), phosphorylated (p-) and total Mek and Erk, and actin as a loading control from lysates derived from **(d)** the head of flies with the indicated versions of transgenic *Ras*^{V12} or **(e)** S2 cells stably transduced with expression vectors expressing the indicated *Ras*^{V12} transgenes. First lane is S2 cells without any transfection.

Figure S2. Rps21 suppresses low Ras signaling. (a, b, c) Immunoblot detection of transgenic Ras^{V12} (with an anti-FLAG antibody), phosphorylated (p-) and total Mek and/or Erk, RpS21, and actin as a loading control from lysates derived from **(a)** the head of flies with the indicated versions of transgenic *Ras*^{V12} in either the wild-type (+/+) or mutant (RpS21^{0375}/+) RpS21 backgrounds, **(b)**

S2 cells stably transduced with expression vectors expressing the indicated Ras^{V12} transgenes in the absence (-) and presence (+) of *RpS21 RNAi* (Data represent two independent replicates.) or **(c)** KC cells stably transduced with expression vectors expressing indicated RasV12 transgenes in the absence (-) and presence (+) of *RpS21 RNAi*. **(d)** The mean ± SEM severity score of the genotypes from three replicate experiments at 18°C, 25°C, and 29°C. Tukey's multiple comparisons test was used for statistical comparisons. . *p<0.05. n.s., not significant.

Figure S3. RpS21 expression is elevated by MAPK signaling. (a,b) Immunoblot detection of Ras, Mek, RpS21, Raf, or actin as a loading control in S2 cells stably transduced with expression vectors expressing **(a)** no transgene (-), activated Mek^{EE}, or activated Ras^{V12} or **(b)** no transgene (-) or activated Raf^{ED} (anti-Pyo antibody to detect tagged *pyo-*Raf^{ED}). **(c)** Immunoblot detection of transgenic Ras^{V12} (with an anti-FLAG antibody), phosphorylated (p-) and total Erk, RpS21, and actin as a loading control from lysates derived from KC cells stably transduced with expression vectors expressing the indicated Ras^{V12} transgenes in the absence (-) and presence of the Mek inhibitor trametinib (Tram). **(d)** Immunoblot detection of transgenic Ras^{V12} (with an anti-FLAG antibody), RpS21, and actin as a loading control from lysates derived from the head of flies with the indicated versions of transgenic Ras^{V12}. **(e)** Immunoblot detection of phosphorylated (p-) and total Mek and Erk, RpS21, and actin as a loading control from lysates derived from serum-starved KC cells at the indicated times after stimulation with fetal bovine serum (FBS).

a

UAS 5X	Flag 3X	Ras^{V12} Rare	attB PhiC
UAS 5X	Flag 3X	Ras^{V12} Common	attB PhiC
UAS 5X	Flag 3X	Ras^{V12} Native	attB PhiC

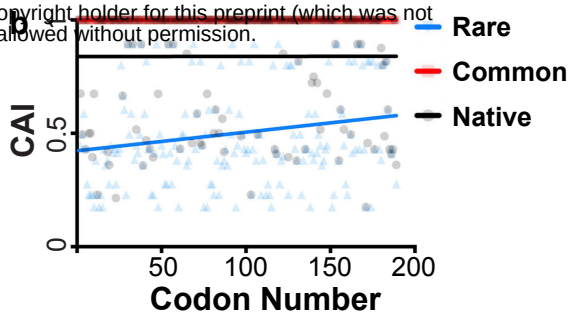

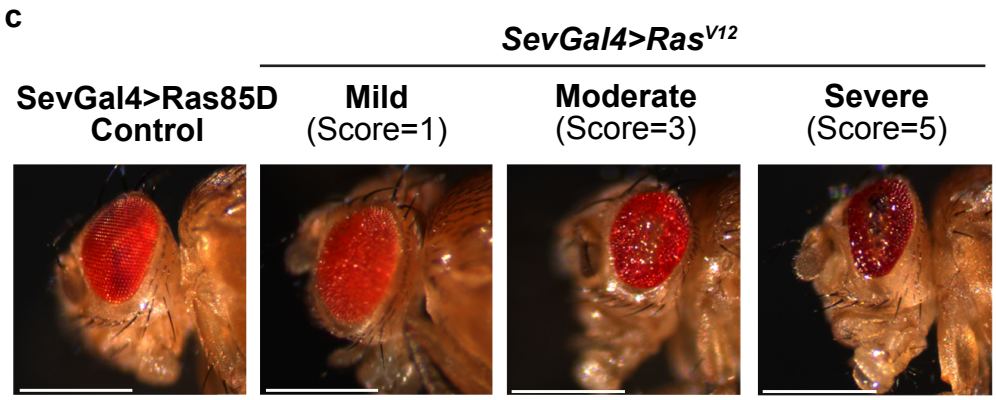

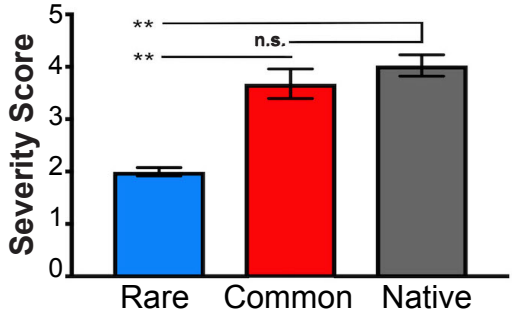

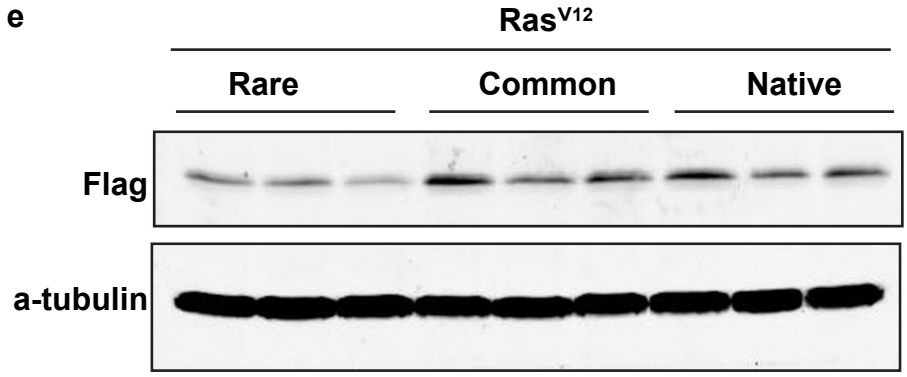

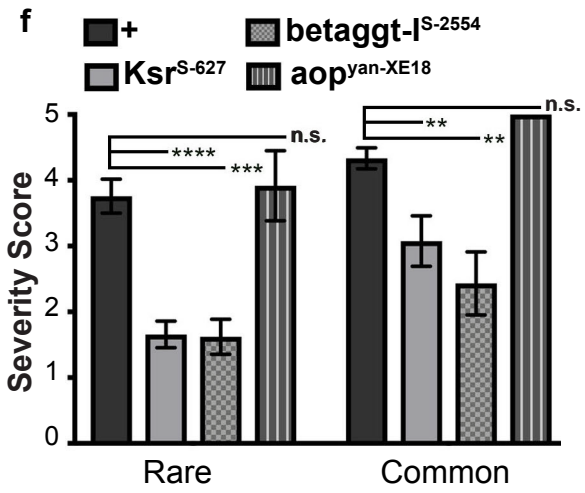

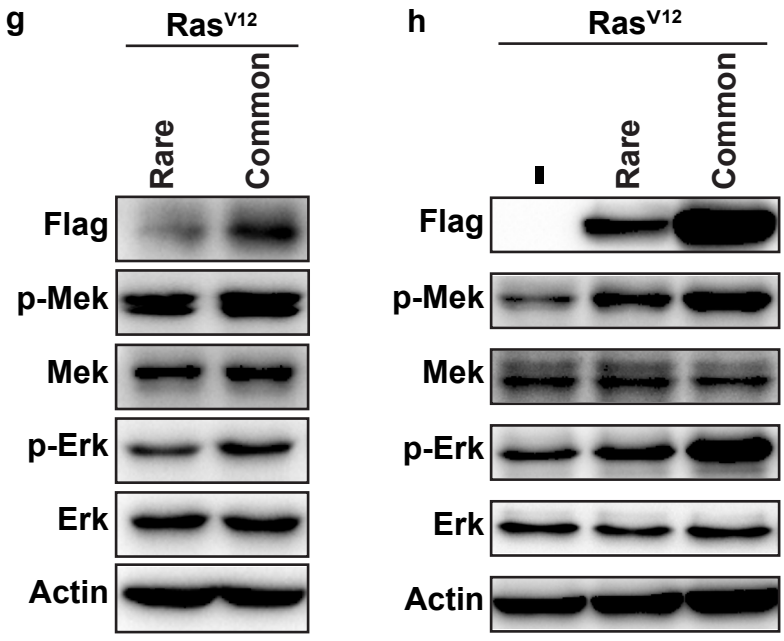

Figure 1.

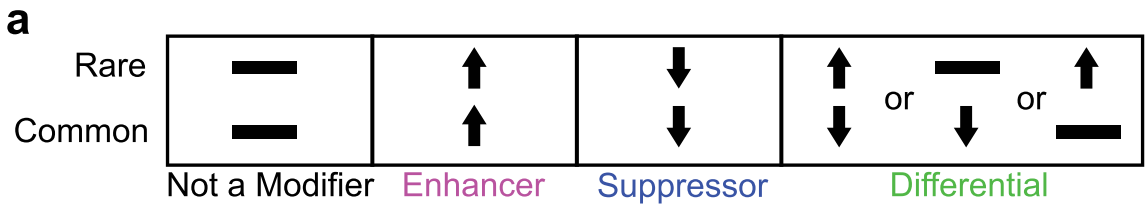

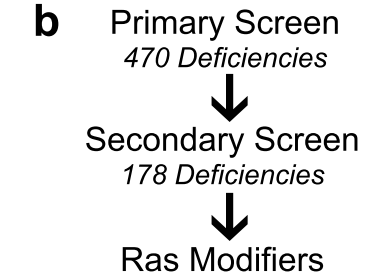

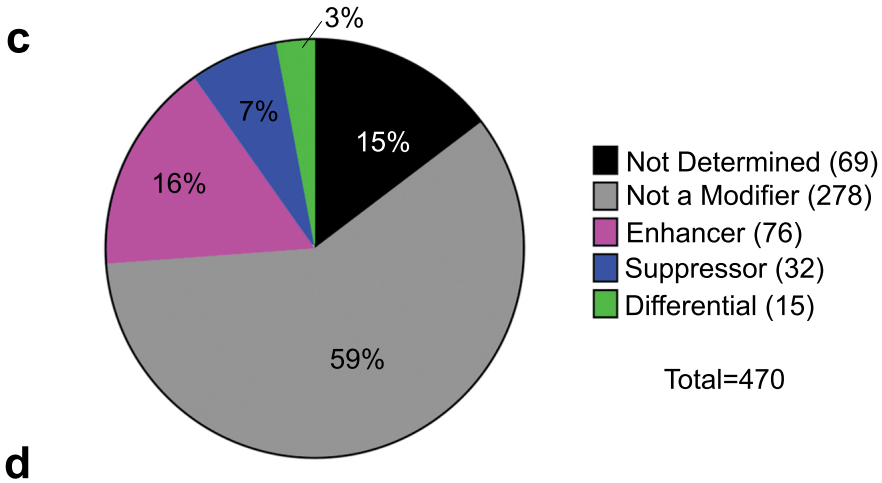

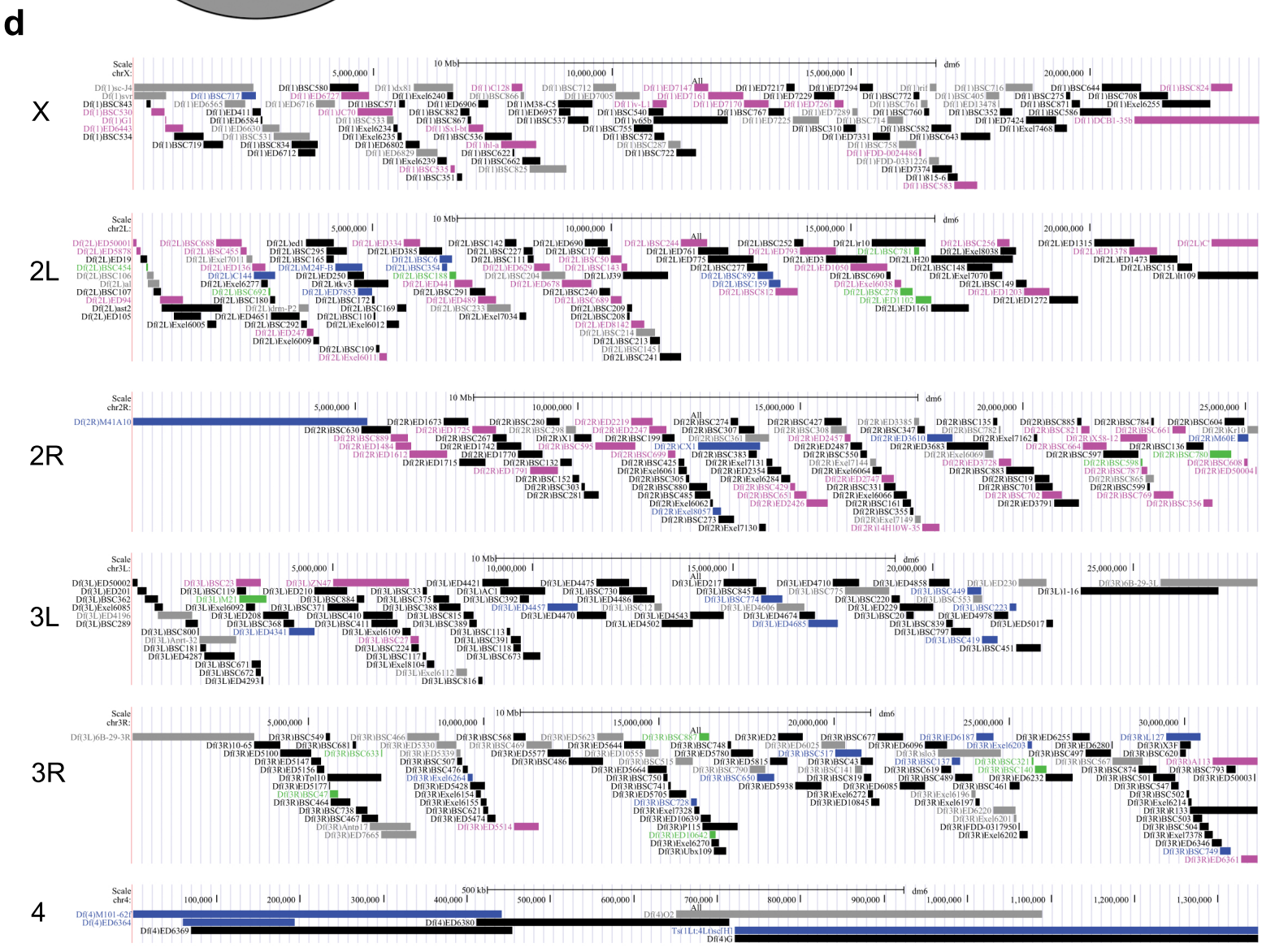

a

Deficiency	Location: Coordinates	Location: Chromosome	Number of Genes	Type of Differential
*Df(2L)BSC454	271351..307085	2L	16	Enhancer of Common
*Df(2L)BSC692	2830265..2868633	2L	12	Enhancer of Rare
*Df(2L)BSC188	6612189..6742726	2L	27	Enhancer of Common
*Df(2L)BSC278	16025369..16289284	2L	25	Enhancer of Rare
Df(2L)ED1102	16350236..16684883	2L	32	Enhancer of Rare
*Df(2L)BSC781	16325113..16417726	2L	13	Enhancer of Rare
*Df(2R)BSC598	22641779..22678681	2R	25	Enhancer of Common
Df(2R)BSC780	24203216..24685191	2R	91	Enhancer of Rare
*Df(3L)M21	2674593..3336860	3L	114	Suppressor of Common
Df(3R)BSC47	5632351..5861298	3R	52	Enhancer of Rare
*Df(3R)BSC633	7080388..7123376	3R	9	Enhancer of Common
*Df(3R)ED10642	16453757..16625271	3R	30	Enhancer of Common
*Df(3R)BSC887	16158034..16442926	3R	51	Suppressor of Rare
*Df(3R)BSC321	25637827..25680519	3R	13	Enhancer of Rare
Df(3R)BSC140	25735650..26055884	3R	77	Suppressor of Common

b

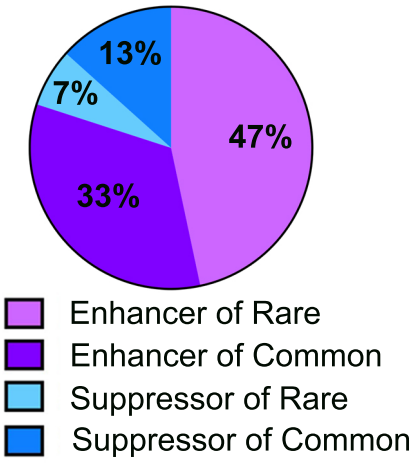

c

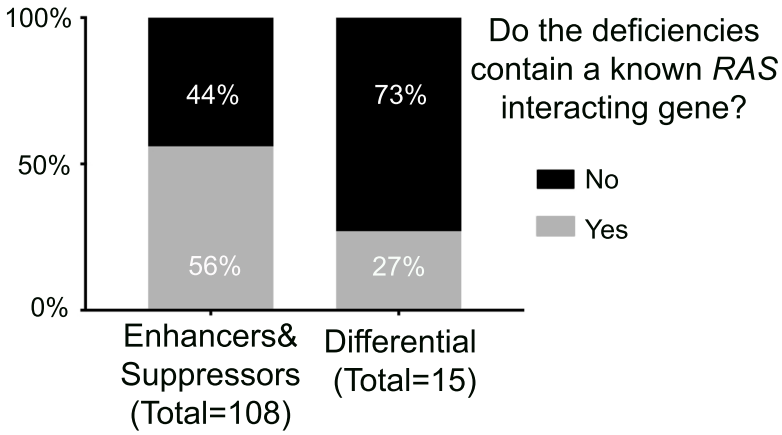

d

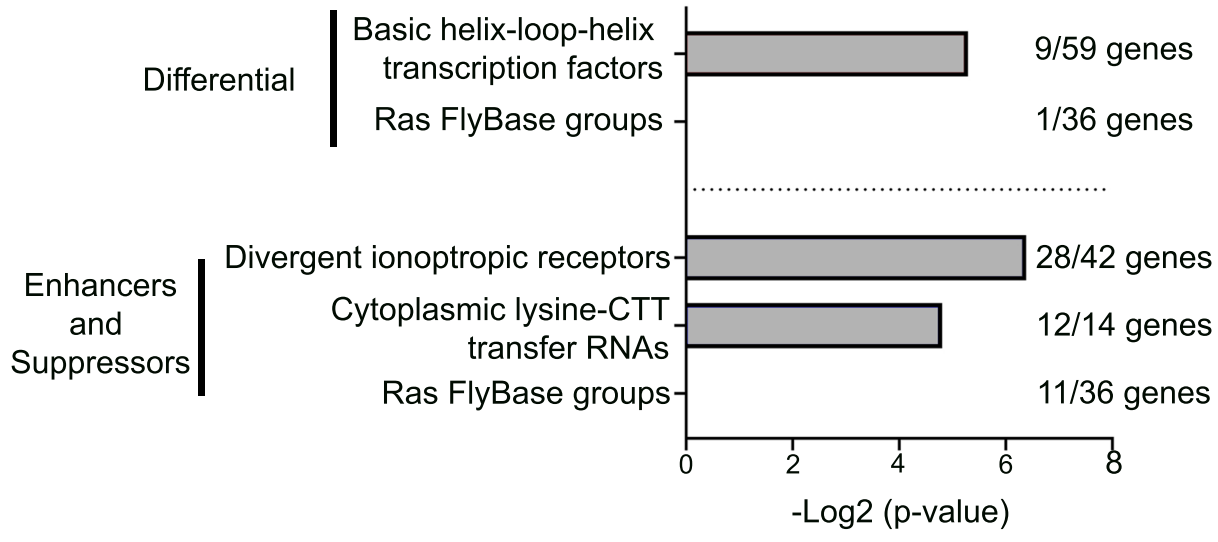

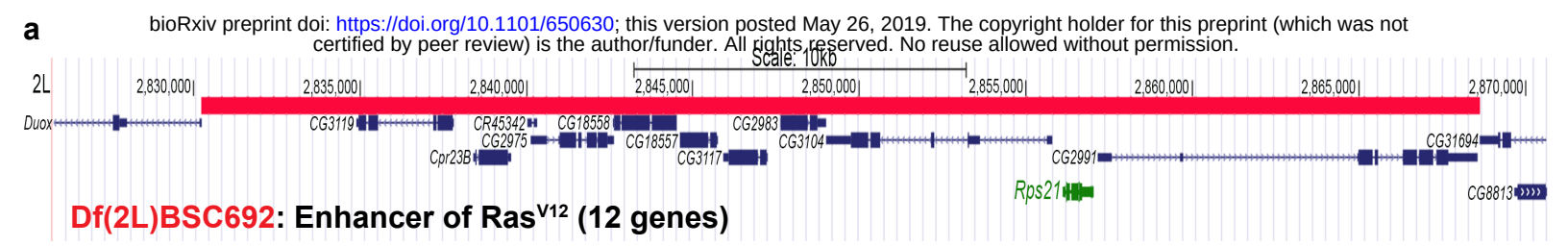

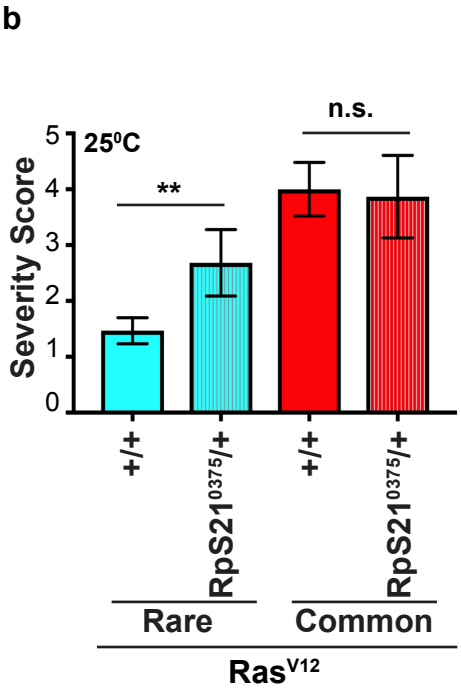

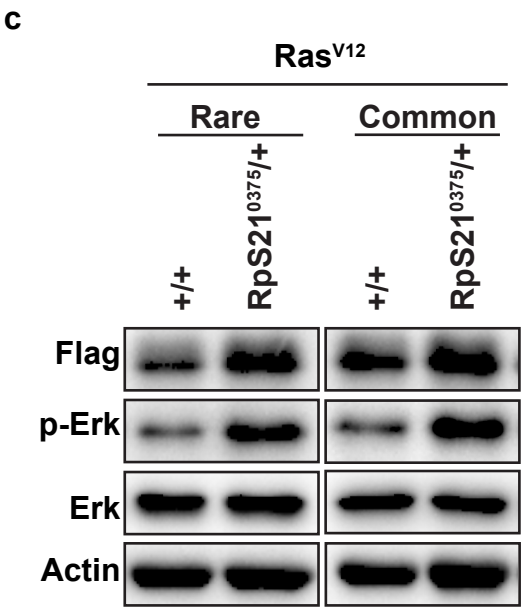

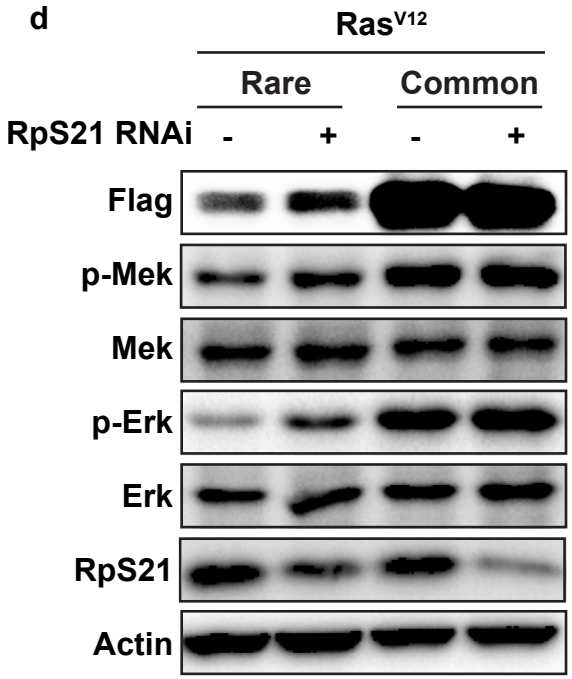

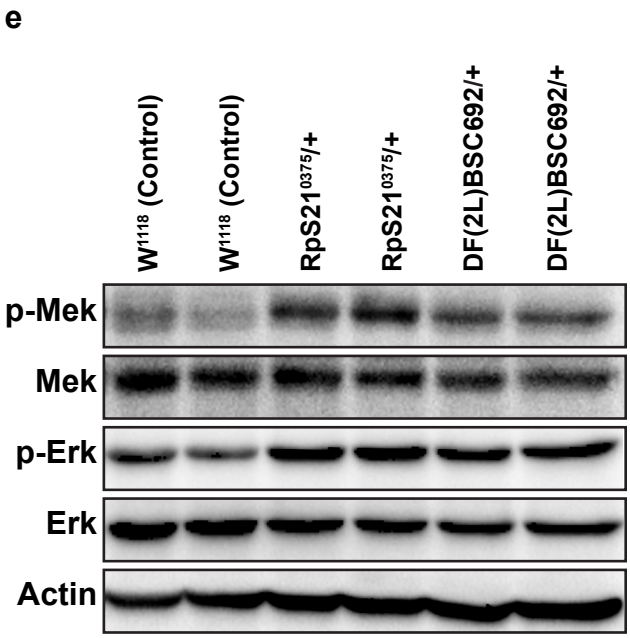

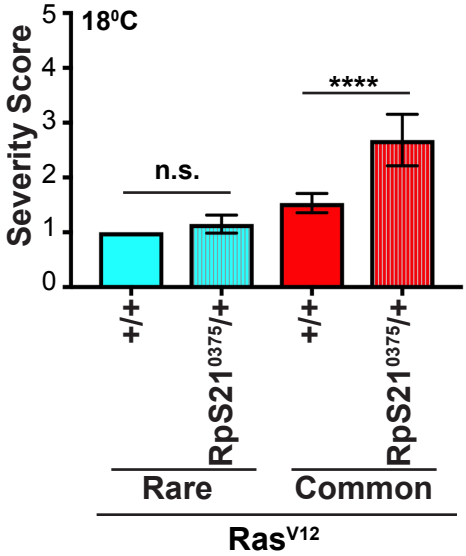

Figure 4.

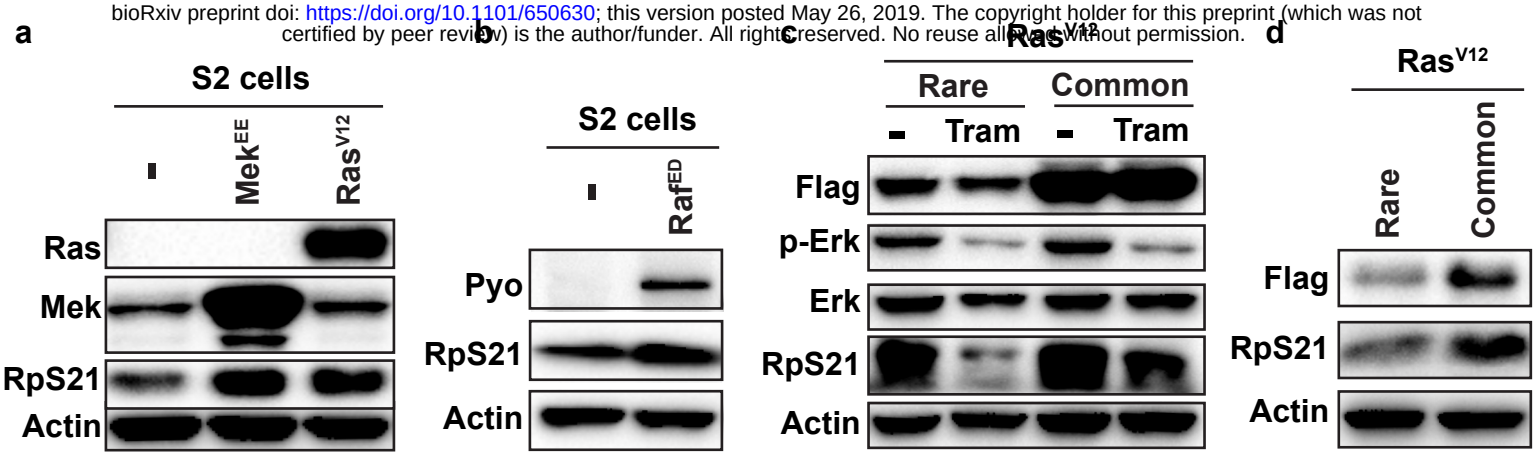

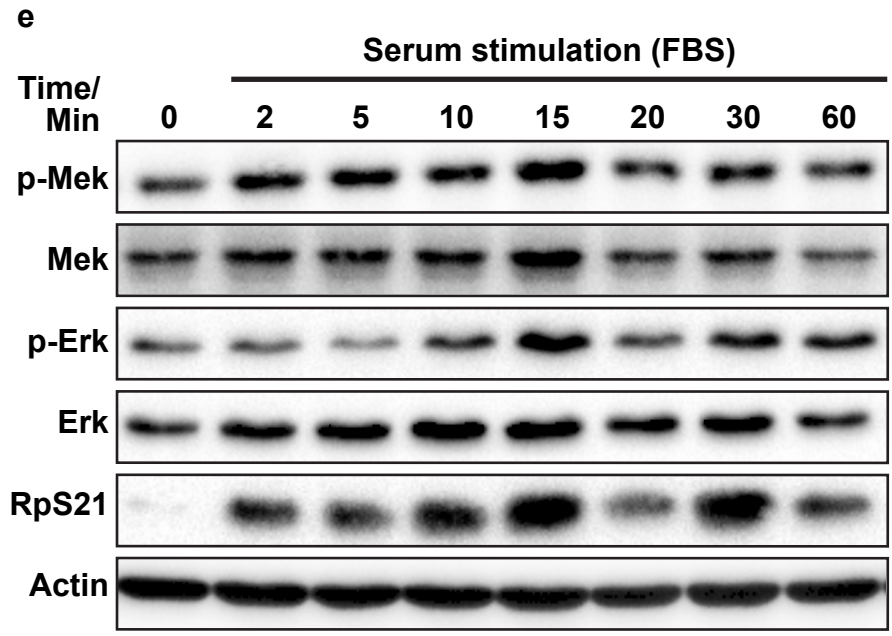

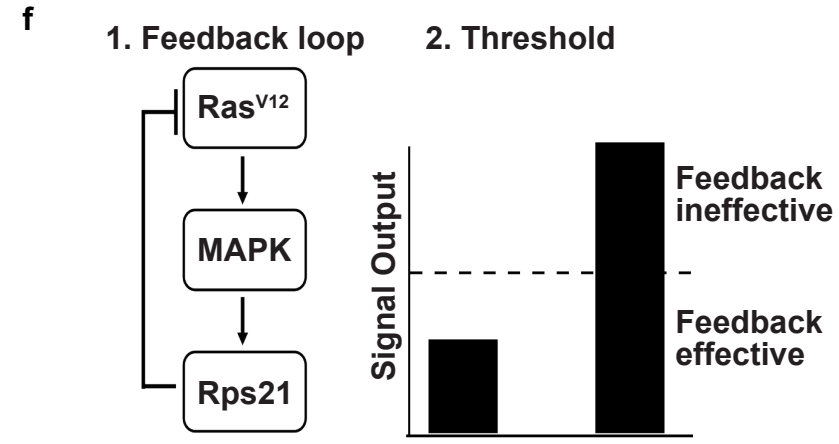

Figure 5.

a

```
                M   T   E   Y   K   L   V   V   V   G   A   V   G   V   G   K   S   A   L   T

Native          ATG ACG GAA TAC AAA CTG GTC GTC GTT GGA GCC GTA GGC GTG GGC AAG TCC GCG CTC ACC   60
Common          ATG ACC GAG TAC AAG CTG GTG GTG GTG GGC GCC GTG GGC GTG GGC AAG AGC GCC CTG ACC
Rare            ATG ACT GAA TAT AAA TTA GTA GTA GTA GGG GCA GTA GGG GTA GGG AAA TCT GCA TTA ACT

                I   Q   L   I   Q   N   H   F   V   D   E   Y   D   P   T   I   E   D   S   Y

Native          ATC CAG CTA ATC CAG AAC CAT TTC GTG GAC GAG TAC GAC CCC ACA ATC GAG GAC TCT TAC  120
Common          ATC CAG CTG ATC CAG AAC CAC TTC GTG GAT GAG TAC GAT CCC ACC ATC GAG GAT AGC TAC
Rare            ATA CAA TTA ATA CAA AAT CAT TTT GTA GAC GAA TAT GAC CCT ACT ATA GAA GAC TCT TAT

                R   K   Q   V   V   I   D   G   E   T   C   L   L   D   I   L   D   T   A   G

Native          CGA AAG CAA GTG GTT ATC GAT GGA GAG ACC TGC CTG CTG GAC ATC CTG GAC ACC GCC GGC  180
Common          CGC AAG CAG GTG GTG ATC GAT GGC GAG ACC TGC CTG CTG GAT ATC CTG GAT ACC GCC GGC
Rare            AGA AAA CAA GTA GTA ATA GAC GGG GAA ACT TGT TTA TTA GAC ATA TTA GAC ACT GCA GGG

                Q   E   E   Y   S   A   M   R   D   Q   Y   M   R   T   G   E   G   F   L   L

Native          CAA GAG GAG TAC TCG GCC ATG CGG GAT CAG TAT ATG CGG ACT GGC GAG GGA TTC CTG CTG  240
Common          CAG GAG GAG TAC AGC GCC ATG CGC GAT CAG TAC ATG CGC ACC GGC GAG GGC TTC CTG CTG
Rare            CAA GAA GAA TAT TCT GCA ATG AGA GAC CAA TAT ATG AGA ACT GGG GAA GGG TTT TTA TTA

                V   F   A   V   N   S   A   K   S   F   E   D   I   G   T   Y   R   E   Q   I

Native          GTC TTT GCC GTC AAC AGT GCG AAG TCC TTC GAG GAT ATC GGC ACC TAC CGT GAG CAG ATC  300
Common          GTG TTC GCC GTG AAC AGC GCC AAG AGC TTC GAG GAT ATC GGC ACC TAC CGC GAG CAG ATC
Rare            GTA TTT GCA GTA AAT TCT GCA AAA TCT TTT GAA GAC ATA GGG ACT TAT AGA GAA CAA ATA

                K   R   V   K   D   A   E   E   V   P   M   V   L   V   G   N   K   C   D   L

Native          AAG CGC GTA AAG GAT GCC GAA GAG GTG CCC ATG GTG CTG GTG GGC AAC AAA TGT GAT CTG  360
Common          AAG CGC GTG AAG GAT GCC GAG GAG GTG CCC ATG GTG CTG GTG GGC AAC AAG TGC GAT CTG
Rare            AAA AGA GTA AAA GAC GCA GAA GAA GTA CCT ATG GTA TTA GTA GGG AAT AAA TGT GAC TTA

                A   S   W   N   V   N   N   E   Q   A   R   E   V   A   K   Q   Y   G   I   P

Native          GCC TCG TGG AAC GTT AAC AAC GAG CAG GCA AGA GAG GTG GCC AAA CAG TAC GGC ATT CCA  420
Common          GCC AGC TGG AAC GTG AAC AAC GAG CAG GCC CGC GAG GTG GCC AAG CAG TAC GGC ATC CCC
Rare            GCA TCA TGG AAT GTA AAT AAT GAA CAA GCA AGA GAA GTA GCA AAA CAA TAT GGG ATA CCT

                Y   I   E   T   S   A   K   T   R   M   G   V   D   D   A   F   Y   T   L   V

Native          TAC ATT GAG ACA TCC GCC AAG ACG CGC ATG GGC GTG GAC GAT GCA TTT TAC ACA CTG GTG  480
Common          TAC ATC GAG ACC AGC GCC AAG ACC CGC ATG GGC GTG GAT GAT GCC TTC TAC ACC CTG GTG
Rare            TAT ATA GAA ACT TCT GCA AAA ACT AGA ATG GGG GTA GAC GAC GCA TTT TAT ACT TTA GTA

                R   E   I   R   K   D   K   D   N   K   G   R   R   G   R   K   M   N   K   P

Native          CGC GAA ATC CGC AAG GAC AAG GAC AAC AAG GGG CGG AGG GGC CGC AAA ATG AAC AAG CCG  540
Common          CGC GAG ATC CGC AAG GAT AAG GAT AAC AAG GGC CGC CGC GGC CGC AAG ATG AAC AAG CCC
Rare            AGA GAA ATA AGA AAA GAC AAA GAC AAT AAA GGG AGA AGA GGG AGA AAA ATG AAT AAA CCT

                N   R   R   F   K   C   K   M   L   STOP

Native          AAT CGT AGA TTT AAA TGT AAA ATG CTC TAA  570
Common          AAC CGC CGC TTC AAG TGC AAG ATG CTG TAA
Rare            AAT AGA AGA TTT AAA TGT AAA ATG TTA TAA
```

Name	Length	CAI	%GC	%GC1	%GC2	%GC3
Native	567	0.782	54.9	57.1	33.9	73.5
Common	567	1.000	61.7	58.7	33.9	92.6
Rare	567	0.432	32.5	45.0	33.9	18.5

b

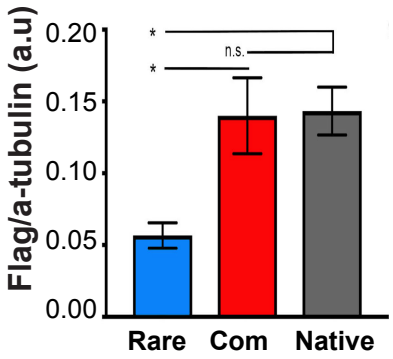

c

	Rare Avg # flies eclosed ±SEM (replicate experiments)	Common Avg # flies eclosed ±SEM (replicate experiments)
+	39±9 (11)	11±4 (11)
ksr^{S-627}	21±4 (7)	15±3 (7)
betaggt-I^{S-2554}	33±14 (4)	29±13 (3)
aop$^{yan-XE18}$	4±3(4)	0±0 (4)

d

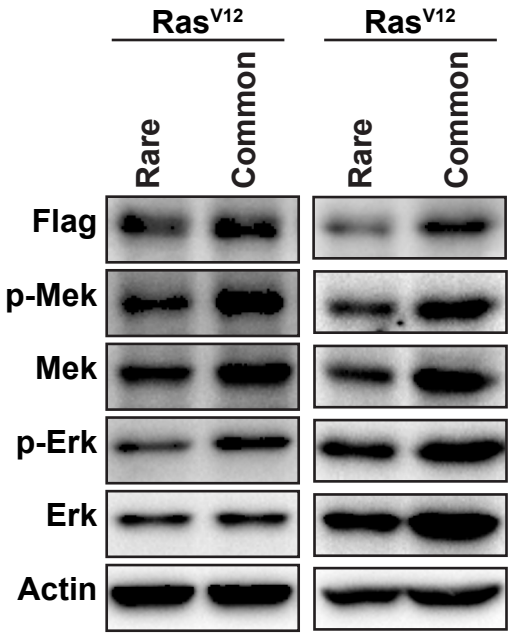

e

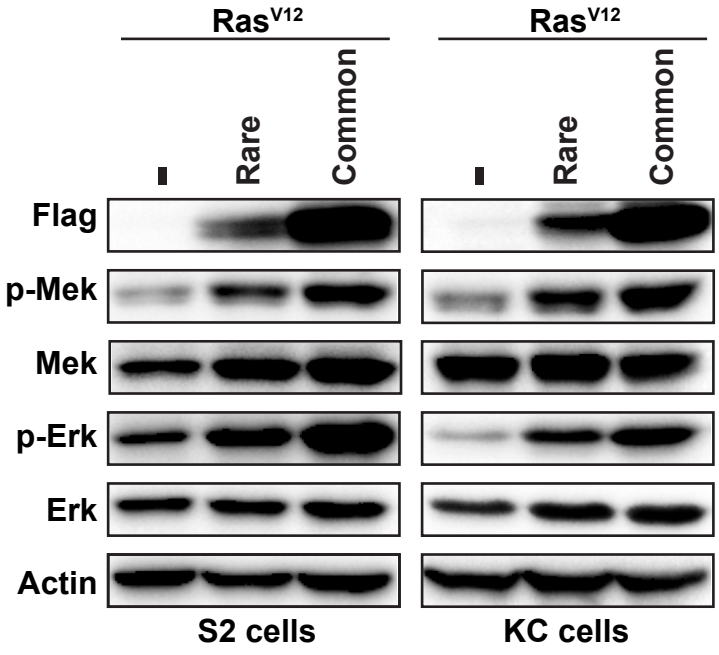

Figure S1.

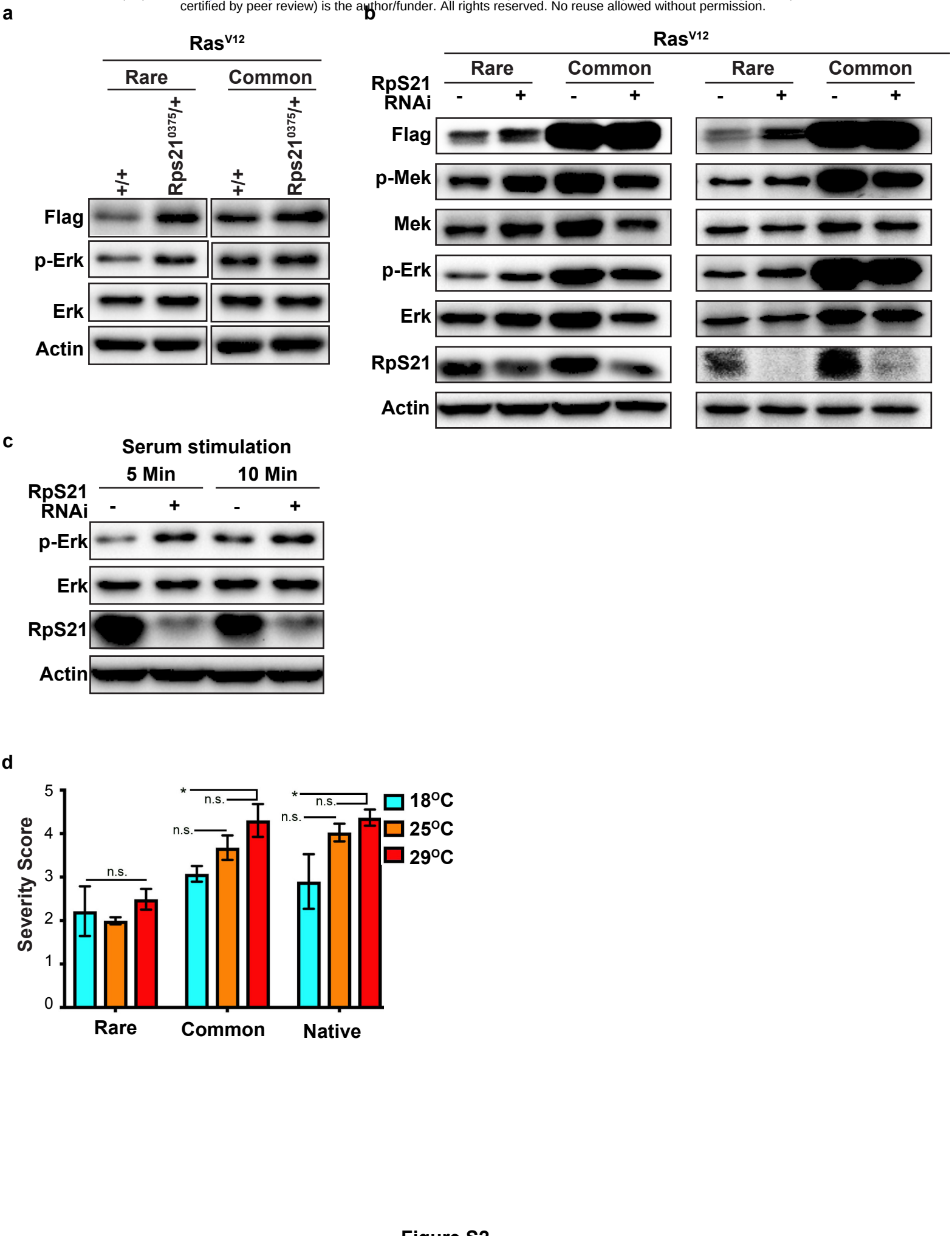

Figure S2.

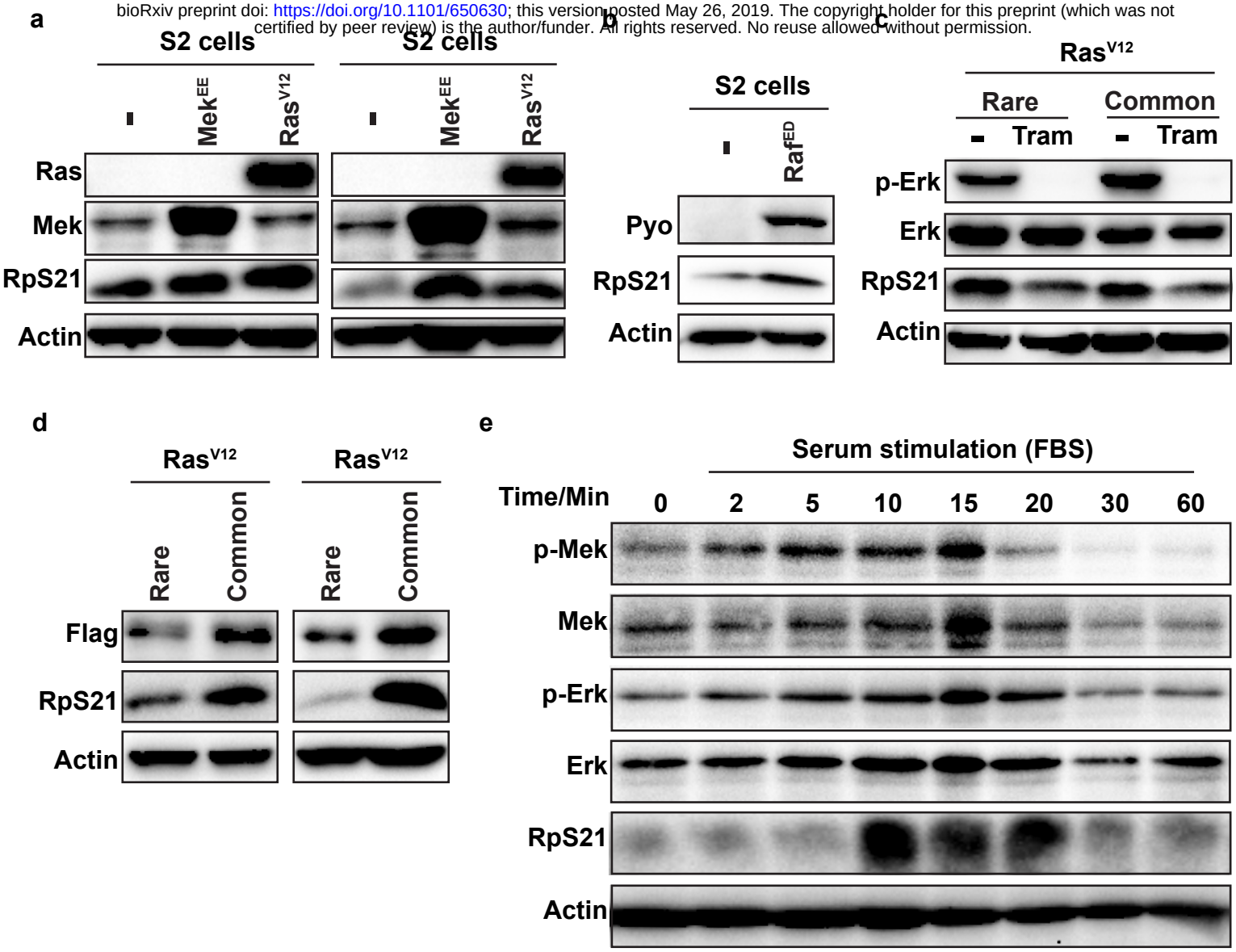

Figure S3.